

# Nuclear-structure contribution to the Lamb shift in muonic deuterium

Carl E. Carlson

*College of William and Mary, Physics Department, Williamsburg, Virginia 23187, USA*

Mikhail Gorchtein\* and Marc Vanderhaeghen

*Institut für Kernphysik, Johannes Gutenberg-Universität, Mainz, Germany**and PRISMA Cluster of Excellence, Johannes Gutenberg-Universität, Mainz, Germany*

(Received 3 December 2013; published 4 February 2014)

We consider the two-photon exchange contribution to the  $2P - 2S$  Lamb shift in muonic deuterium in the framework of forward dispersion relations. The dispersion integrals are evaluated using experimental data on elastic deuteron form factors and inelastic electron-deuteron scattering, both in the quasielastic and hadronic range. The subtraction constant that is required to ensure convergence of the dispersion relation for the forward Compton amplitude  $T_1(\nu, Q^2)$  is related to the deuteron magnetic polarizability  $\beta(Q^2)$ . Based on phenomenological information, we obtain for the Lamb shift  $\Delta E_{2P-2S} = 2.01 \pm 0.74$  meV. The main source of the uncertainty of the dispersion analysis is due to lack of quasielastic data at low energies and forward angles. We show that a targeted measurement of the deuteron electrodesintegration in the kinematics of upcoming experiments A1 and MESA at Mainz can help in quenching this uncertainty significantly.

DOI: [10.1103/PhysRevA.89.022504](https://doi.org/10.1103/PhysRevA.89.022504)

PACS number(s): 31.30.jr, 13.40.Gp, 14.20.Dh, 36.10.Ee

## I. INTRODUCTION

The proton radius puzzle—that the proton radius obtained from the Lamb shift in muonic hydrogen [1,2] is different from what should be the same radius obtained from data involving electrons [3,4]—has attracted much attention in recent years. The explanation of the problem is not known so far. There are proposals of new dedicated scattering experiments with electrons [5,6] and muons [7]. On the theory side, the discrepancy was addressed in terms of effective nonrelativistic QED interactions [8], dispersion relations [9], exotically large hadronic effects [10], or of new physics affecting the muon and electron differently [11–13].

Further information can come from measuring the deuteron radius using the Lamb shift in muonic deuterium [14]. The deuteron radius from electron based experiments is already known to good accuracy. The best results come from using the isotope shift, that is, measuring the  $1S$ - $2S$  splittings in electron-proton ( $e$ - $H$ ) and electron-deuteron ( $e$ - $D$ ) hydrogen and finding from residual corrections that

$$r_E^2(d) - r_E^2(p) = 3.820\,07(65) \text{ fm}^2, \quad (1)$$

as quoted in [15,16], where the  $r_E(p, d)$  are charge radii. The isotope shift number is so accurate that the uncertainty in the deuteron radius squared becomes in practice the same as for the proton, and using the CODATA 2010 value for the proton radius one finds [3]

$$r_E(d) = 2.1424(21) \text{ fm}. \quad (2)$$

The uncertainty is 0.1%. In contrast, the current best direct electron-deuteron scattering results yield  $r_E(d) = 2.128(11)$  fm [17], or 0.5% uncertainty. Planned experiments are expected to reduce this uncertainty [18].

To obtain the charge radius from the Lamb shift requires not only accurate data but also accurate calculation of all

corrections that are not hadronic size corrections. Of these, the two-photon correction, which includes the relativistically correct polarizability correction, has drawn continued attention. A deuteron is easily distorted compared to a single proton, and we shall see that the polarizability correction for the  $\mu$ - $D$  system is about two orders of magnitude larger than for  $\mu$ - $H$ . The requirement that the  $\mu$ - $D$  polarizability correction be safely smaller than the radius-related energy shift can become quite severe.

Of course, without knowing the underlying reason for the proton radius discrepancy, we cannot with certainty predict what the deuteron discrepancy will be. However, we will give the anticipated energy discrepancy in one scenario, and thereby obtain a working number with the expectation that other scenarios would give results similar within a factor of a few. As a reminder, the main energy shift due to finite hadron (or nuclear) size is

$$\Delta E_{\text{finite size}} = \frac{2\pi Z\alpha}{3} \frac{(m_r Z\alpha)^3}{n^3\pi} r_E^2(h), \quad (3)$$

for a hydrogenlike atom in the  $nS$  state, where  $m_r$  is the reduced mass. Experiment shows about a  $320$ - $\mu\text{eV}$  energy discrepancy for the  $\mu$ - $H$   $2S$  state, compared to expectations based on the CODATA 2010 [3] electron based proton radius.

In a scenario where the  $\mu$ - $H$  energy discrepancy is not actually due to a proton size change but rather to the exchange of a new particle that has a special coupling to the muon and, e.g., a dark photon coupling (i.e., a squelched electromagnetic coupling) to other particles, the  $\mu$ - $D$  energy would be the same as in the  $\mu$ - $H$  except for the reduced-mass-cubed factor. In this case the anticipated  $\mu$ - $D$  energy discrepancy is

$$\Delta E_{\text{discrepant}}(\mu-D) \approx 380 \mu\text{eV}. \quad (4)$$

Hence the two-photon corrections should be calculated within  $100 \mu\text{eV}$  or less. As the two-photon corrections are of order  $2$  meV, this requires a 5% or better accuracy.

\*gorshtey@kph.uni-mainz.de

There are several currently available polarizability calculations [19–24]. Reference [19] includes the elastic contributions and quotes an uncertainty limit well within the requirement. A more recent calculation of Ref. [24] follows the same lines but includes further relativistic corrections. In addition, much of that calculation is supported by a calculation [23] that uses the zero-range approximation which indicates that the bulk of the result is relatively model independent and can be obtained nonrelativistically. However, there remain significant energy shifts that are obtained nonrelativistically using a potential model. One would like a calculation by an alternative method to verify the results.

We here explore a fully relativistic dispersive calculation of the two-photon corrections to  $\mu$ - $D$ . In this type of calculation, the energy shift is obtained from the real part of an amplitude whose imaginary part is related without approximation to physical elastic and inelastic  $e$ - $D$  scattering. To the extent that the data are accurate and sufficient, the result follows just from the data and the calculation is model independent. The calculation resembles the generally accepted work for the  $\mu$ - $H$  system [25–29]. However, for the proton case the corrections are much smaller, and the proton data in the relevant kinematic regions is itself very good. Furthermore, good analytic fits, useful for doing integrals, are already available in the literature [30].

For the deuteron we need elastic and inelastic data over a wide range of energies, including the low-energy region, where the data are sparse. There are good analytic fits [31] to the deuteron data above the pion production threshold, but not in the lower energy quasielastic region. Part of our effort is devoted to providing such fits. The inelastic data are represented in terms of structure functions or response functions. The overall polarizability effect is sensitive to the structure of the response functions at low energy and low virtual photon masses, which is where the data are sparse. A consequence of this, phrased in terms of fitting procedures, is that small changes in some parameters have big effects on the near threshold behavior but small effect on the quality of the fits to the available data. This leads to a larger than desired uncertainty in the results for the two-photon corrections, when using this method.

Future low momentum transfer deuteron breakup data, possibly obtained as background data to elastic-scattering experiments [18], can bring about a decisive reduction in the uncertainty limits of the polarizability calculation. We discuss this below with some examples.

Our presentation starts with the description of the general dispersive formalism for obtaining energy shifts from elastic and inelastic-scattering data and subtraction terms in Sec. II. Evaluation of the elastic and inelastic dispersion integrals is discussed in Sec. III where we as well provide details of our global fit to the available quasielastic deuteron data. In Sec. IV we present our results, discuss the uncertainty limits, and address possible help from upcoming experiments. Section V is dedicated to the application of the dispersive, data-based, model-independent polarizability calculation described here to the  $e$ - $H$  and  $e$ - $D$  systems and its relevance to the isotope shift measurements. Section VI closes the article with a short summary of our findings.

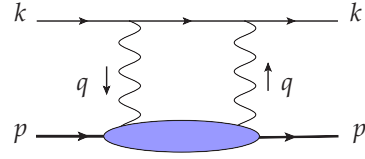


FIG. 1. (Color online) Two-photon exchange diagram for the  $O(\alpha^5)$  correction to the Lamb shift.

## II. BASIC FORMALISM

The diagram that contains the nuclear and hadronic structure-dependent  $O(\alpha^5)$  correction to the Lamb shift is shown in Fig. 1. In the lower part of the diagram, the blob containing the nuclear and hadronic structure dependence is encoded in the forward virtual Compton tensor,

$$\begin{aligned} T^{\mu\nu} &= \frac{i}{8\pi M_d} \int d^4x e^{iqx} \langle p | T j^\mu(x) j^\nu(0) | p \rangle \\ &= \left( -g^{\mu\nu} + \frac{q^\mu q^\nu}{q^2} \right) T_1(\nu, Q^2) + \frac{\hat{p}^\mu \hat{p}^\nu}{M_d^2} T_2(\nu, Q^2), \end{aligned} \quad (5)$$

where  $\hat{p}^\mu = p^\mu - \frac{p \cdot q}{q^2} q^\mu$ ,  $Q^2 = -q^2$ ,  $\nu = (p \cdot q)/M_d$ , and  $M_d$  is the deuteron mass. Following [27], we can write the contribution of the two-photon exchange diagram to the  $n\ell$  energy level as

$$\begin{aligned} \Delta E_{n\ell} &= \frac{8\alpha^2 m}{\pi} \phi_{n\ell}^2(0) \int d^4Q \\ &\times \frac{(Q^2 + 2Q_0^2) T_1(iQ_0, Q^2) - (Q^2 - Q_0^2) T_2(iQ_0, Q^2)}{Q^4 (Q^4 + 4m^2 Q_0^2)}, \end{aligned} \quad (6)$$

where a Wick rotation  $q_0 = iQ_0$  was made, and  $\phi_{n\ell}^2(0) = \mu_r^3 \alpha^3 / (\pi n^3) \delta_{\ell 0}$ ,  $\mu_r = mM/(M+m)$  being the reduced mass.  $T_{1,2}(\nu, Q^2)$  are even functions of  $\nu$  and their imaginary parts are related to the spin-independent structure functions of lepton-deuteron scattering,

$$\text{Im} T_1(\nu, Q^2) = \frac{1}{4M_d} F_1(\nu, Q^2), \quad (7)$$

$$\text{Im} T_2(\nu, Q^2) = \frac{1}{4\nu} F_2(\nu, Q^2).$$

Given the known high-energy behavior of the structure functions, the two amplitudes obey the following form of dispersion relation:

$$\begin{aligned} \text{Re} T_1(q_0, Q^2) &= \bar{T}_1(0, Q^2) + \text{Re} T_1^{\text{pole}}(q_0, Q^2) \\ &+ \frac{q_0^2}{2\pi M_d} \int_{\nu_{thr}}^{\infty} \frac{d\nu F_1(\nu, Q^2)}{\nu(\nu^2 - q_0^2)}, \\ \text{Re} T_2(q_0, Q^2) &= \text{Re} T_2^{\text{pole}}(q_0, Q^2) + \frac{1}{2\pi} \int_{\nu_{thr}}^{\infty} \frac{d\nu F_2(\nu, Q^2)}{\nu^2 - q_0^2}, \end{aligned} \quad (8)$$

where for  $T_1$  the subtraction at  $q_0 = 0$  was performed with  $\bar{T}_1(0, Q^2)$  the respective subtraction function. Above, we explicitly extracted the contribution of the ground state leading to a pole,  $T_{1,2}^{\text{pole}}$ . This contribution is defined in terms of the

deuteron's electromagnetic vertex

$$\begin{aligned} & \langle d(p') | J^\mu(q) | d(p) \rangle \\ &= G_2(Q^2) [\xi'^{\mu}(\xi q) - \xi^\mu(\xi' q)] \\ & - \left[ G_1(Q^2)(\xi'^{\mu} \xi) - G_3(Q^2) \frac{(\xi'^{\mu} q)(\xi q)}{2M_d^2} \right] (p + p')^\mu, \quad (9) \end{aligned}$$

where  $\xi^\mu(\xi'^{\mu})$  denote the polarization vector of the initial (final) deuteron with momenta  $p(p')$ , respectively, and  $Q^2 = -q^2$  stands for the four-momentum transfer. The form factors  $G_{1,2,3}$  are related to the charge, magnetic, and quadrupole deuteron form factors as

$$\begin{aligned} G_M &= G_2, \\ G_C &= G_1 + \frac{2}{3} \tau_d G_Q, \\ G_Q &= G_1 - G_2 + (1 + \tau_d) G_3, \end{aligned} \quad (10)$$

and  $\tau_d = Q^2/(4M_d^2)$ . The elastic contribution to the structure functions reads

$$\begin{aligned} F_1^{el} &= \frac{1}{3}(1 + \tau_d) G_M^2 \delta(1 - x_d), \\ F_2^{el} &= [G_C^2 + \frac{2}{3} \tau_d G_M^2 + \frac{8}{9} \tau_d^2 G_Q^2] \delta(1 - x_d), \end{aligned} \quad (11)$$

with the Bjorken variable  $x_d = Q^2/(2M_d v)$ .

Correspondingly, we distinguish three contributions,  $\Delta E_{n0} = \Delta E_{n0}^{\text{subt}} + \Delta E_{n0}^{el} + \Delta E_{n0}^{\text{inel}}$  where

$$\Delta E_{n0}^{\text{subt}} = \frac{4\pi\alpha^2}{m} \phi_{n0}^2(0) \int_0^\infty \frac{dQ^2}{Q^2} \frac{\gamma_1(\tau_l)}{\sqrt{\tau_l}} \bar{T}_1(0, Q^2), \quad (12)$$

$$\begin{aligned} \Delta E_{n0}^{el} &= \frac{m\alpha^2}{M_d(M_d^2 - m^2)} \phi_{n0}^2(0) \int_0^\infty \frac{dQ^2}{Q^2} \\ & \times \left\{ \frac{2}{3} G_M^2 (1 + \tau_d) \left( \frac{\gamma_1(\tau_d)}{\sqrt{\tau_d}} - \frac{\gamma_1(\tau_l)}{\sqrt{\tau_l}} \right) \right. \\ & \left. - \left( \frac{\gamma_2(\tau_d)}{\sqrt{\tau_d}} - \frac{\gamma_2(\tau_l)}{\sqrt{\tau_l}} \right) \left[ \frac{G_C^2}{\tau_d} + \frac{2}{3} G_M^2 + \frac{8}{9} \tau_d G_Q^2 \right] \right\}, \end{aligned} \quad (13)$$

$$\begin{aligned} \Delta E_{n0}^{\text{inel}} &= -\frac{2\alpha^2}{M_d m} \phi_{n0}^2(0) \int_0^\infty \frac{dQ^2}{Q^2} \int_{v_{thr}}^\infty \frac{dv}{v} \\ & \times \left[ \tilde{\gamma}_1(\tau, \tau_l) F_1(v, Q^2) + \frac{M_d v}{Q^2} \tilde{\gamma}_2(\tau, \tau_l) F_2(v, Q^2) \right]. \end{aligned} \quad (14)$$

Above, we denote  $\tau = v^2/Q^2$ ,  $\tau_l = Q^2/(4m^2)$ , and the auxiliary functions are given by

$$\begin{aligned} \gamma_1(\tau) &= (1 - 2\tau)\sqrt{1 + \tau} + 2\tau^{3/2}, \\ \gamma_2(\tau) &= (1 + \tau)^{3/2} - \tau^{3/2} - \frac{3}{2}\sqrt{\tau}, \\ \tilde{\gamma}_1(\tau, \tau_l) &= \frac{\sqrt{\tau}\gamma_1(\tau) - \sqrt{\tau_l}\gamma_1(\tau_l)}{\tau - \tau_l}, \\ \tilde{\gamma}_2(\tau, \tau_l) &= \frac{1}{\tau - \tau_l} \left[ \frac{\gamma_2(\tau_l)}{\sqrt{\tau_l}} - \frac{\gamma_2(\tau)}{\sqrt{\tau}} \right]. \end{aligned} \quad (15)$$

### III. EVALUATION AND DATA FITS

#### A. Elastic contribution

We start with the elastic contribution. It can be noted that the integral in Eq. (13) is IR divergent due to an exchange of soft Coulomb photons. Such contributions, however, were already taken into account within the nonrelativistic calculations on a pointlike deuteron. Furthermore, the finite-size effects were accounted for, as well, and have to be subtracted from the full result of Eq. (13) to avoid double counting. This subtraction leads to

$$\begin{aligned} \Delta \bar{E}_{n0}^{el} &= \frac{m\alpha^2}{M_d(M_d^2 - m^2)} \phi_{n0}^2(0) \int_0^\infty \frac{dQ^2}{Q^2} \\ & \times \left\{ \frac{2}{3} G_M^2 (1 + \tau_d) \left( \frac{\gamma_1(\tau_d)}{\sqrt{\tau_d}} - \frac{\gamma_1(\tau_l)}{\sqrt{\tau_l}} \right) \right. \\ & \left. - \left( \frac{\gamma_2(\tau_d)}{\sqrt{\tau_d}} - \frac{\gamma_2(\tau_l)}{\sqrt{\tau_l}} \right) \left[ \frac{G_C^2 - 1}{\tau_d} + \frac{2}{3} G_M^2 + \frac{8}{9} \tau_d G_Q^2 \right] \right. \\ & \left. + 16M_d^2 \frac{M_d - m}{Q} G_C'(0) \right\}. \end{aligned} \quad (16)$$

We evaluate Eq. (16) with the most recent deuteron form factors' parametrization from [32]. We use the parametrization I and II of [32] to estimate the uncertainty, and list the result with the uncertainty in Table I.

The inelastic contributions contain two parts,

$$\Delta E_{n0}^{\text{inel}} = \Delta E_{n0}^{QE} + \Delta E_{n0}^{\text{hadr}}, \quad (17)$$

the quasielastic nucleon knock-out (QE) and hadronic excitation spectrum (hadr) that we will treat separately.

#### B. Hadronic contribution

The part of the deuteron excitation spectrum above the pion production threshold can be dealt with very similarly as was done in Ref. [27] for the proton case. We use the modern deuteron virtual photoabsorption data that were parametrized in terms of resonances plus nonresonant background by Bosted and Christy in [30,31]. Since the integration over the energy extends beyond the validity of the fit of Ref. [30,31], we supplement the correct high-energy behavior by adopting a Regge-behaved background. The Regge fit to world data on the deuteron total photoabsorption cross section was done in [29]. We extend this description to virtual photoabsorption by supplementing a  $Q^2$  dependence from generalized VDM, e.g., [33], that provides good description of virtual photoabsorption data at  $Q^2 \lesssim 3 \text{ GeV}^2$ . The result for  $\Delta E^{\text{hadr}}$  is reported in Table I.

#### C. Quasielastic contribution

In the literature, there exist nonrelativistic calculations of the Lamb shift in muonic deuterium with potential models or in zero-range approximations [19–24]. In this work we opt for a phenomenological, data-driven approach in the spirit of Ref. [27] where real and virtual photoabsorption data on the proton were utilized to constrain the Lamb shift in the muonic hydrogen. For this purpose we need to fit the quasielastic data

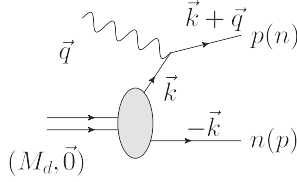


FIG. 2. Quasielastic scattering kinematics.

over the whole kinematical range with an appropriate function of  $\nu$ ,  $Q^2$ .

We start with the plane wave Born approximation (PWBA) that allows us to relate the deuteron structure functions to the elastic nucleon structure functions. In doing this, we Fermi smear the nucleon virtual Compton tensor, rather than just the structure functions; the result reads

$$F_1^{\text{PWBA}} = \frac{Q^2}{4|\vec{q}|} G_M^2 S(\nu, Q^2) + \frac{1}{2|\vec{q}|} \frac{G_E^2 + \tau G_M^2}{1 + \tau} S_{\perp}(\nu, Q^2),$$

$$F_2^{\text{PWBA}} = \frac{\nu Q^2}{2M_d |\vec{q}|^3} \frac{G_E^2 + \tau G_M^2}{1 + \tau} \times \left[ (2M + \nu)^2 \frac{Q^2}{2|\vec{q}|^2} S(\nu, Q^2) + S_{\perp}(\nu, Q^2) \right]. \quad (18)$$

Above, we defined the integrals

$$S(\nu, Q^2) = \int_{k_{\min}}^{k_{\max}} dk k [u^2(p) + w^2(p)], \quad (19)$$

$$S_{\perp}(\nu, Q^2) = \int_{k_{\min}}^{k_{\max}} dk k [u^2(p) + w^2(p)] k_{\perp}^2.$$

The deuteron wave function is normalized as  $\int k^2 dk [u^2(p) + w^2(p)] = 1$ ,  $u, w(p)$  denote the  $s, d$  radial wave function of the deuteron, respectively. The magnitude of the three-momentum of the bound nucleon is denoted by  $k = |\vec{k}|$ , and its component perpendicular to the direction of the virtual photon is  $k_{\perp}^2 = k^2 \sin^2 \theta_k$ ; the angle  $\theta_k$  is defined below. The on-shell condition for the external (knock-out) nucleons and four-momentum conservation

$$M_d + \nu = \sqrt{M^2 + (\vec{q} + \vec{k})^2} + \sqrt{M^2 + \vec{k}^2}, \quad (20)$$

with the average nucleon mass  $M \equiv \frac{1}{2}(M_p + M_n) \approx 0.938919$  GeV, leads to a  $\delta$  function for the angle between the three-momenta of the virtual photon and the active nucleon,

$$\cos \theta_k = \frac{2(M_d + \nu) \sqrt{M^2 + \vec{k}^2} - (M_d + \nu)^2 + |\vec{q}|^2}{2|\vec{q}||\vec{k}|}. \quad (21)$$

The integral over the Fermi momentum  $k$  is constrained between two finite values due to the requirement  $-1 \leq \cos \theta_k \leq 1$ ,

$$k_{\min} = \left| -\frac{|\vec{q}|}{2} + \frac{M_d + \nu}{2} \sqrt{\frac{\nu - \nu_{\min}}{M_d/2 + \nu - \nu_{\min}}} \right|, \quad (22)$$

$$k_{\max} = \frac{|\vec{q}|}{2} + \frac{M_d + \nu}{2} \sqrt{\frac{\nu - \nu_{\min}}{M_d/2 + \nu - \nu_{\min}}},$$

with  $\nu_{\min} = Q^2/(2M_d) + \epsilon + O(\epsilon^2)$  and  $\epsilon = 2M - M_d \approx 2.224$  MeV.

Experimental data on deuteron electrodesintegration feature a sharp peak just above the threshold, that is due to final-state interactions between proton and neutron after the breakup [34]. We adopt an approximate formula [Eq. (48) of [34]] to obtain the following model for the transverse and longitudinal cross sections:

$$\sigma_T^0 = \sqrt{\frac{\nu - \nu_{\min}}{M + \nu - \nu_{\min}}} \frac{[G_M^p(Q^2) - G_M^n(Q^2)]^2}{1 + M(\nu - \nu_{\min})a_S^2}, \quad (23)$$

$$\sigma_L^0 = \sqrt{\frac{\nu - \nu_{\min}}{M + \nu - \nu_{\min}}} \frac{[G_E^p(Q^2) + G_E^n(Q^2)]^2}{1 + M(\nu - \nu_{\min})a_T^2}, \quad (24)$$

with the  $n$ - $p$  singlet and triplet scattering lengths entering the FSI part,  $a_S = -23.74$  fm,  $a_T = 5.38$  fm, respectively. Above, we note that the combination  $\sqrt{M(\nu - \nu_{\min})} = |\vec{p}|$  corresponds to the three-momentum of the knocked-out nucleon.

As a result, we obtain the following representation of the quasielastic structure functions of the deuteron:

$$F_{1,2}^{d, QE} = F_{1,2}^{\perp} + F_{1,2}^{\text{PWBA}} + F_{1,2}^{\text{FSI}}, \quad (25)$$

according to the ingredients discussed above. To describe data at arbitrary kinematics, we allow for a rescaling of each ingredient by a function of  $Q^2$  that should be obtained from the fit to the deuteron photo- and electrodesintegration data.

$$F_1^{\perp} = C_{\perp} \frac{G_E^2 + \tau G_M^2}{1 + \tau} \frac{1}{2|\vec{q}|} S_{\perp}(\nu, Q^2),$$

$$F_2^{\perp} = \frac{\nu Q^2}{M_d |\vec{q}|^2} F_1^{\perp},$$

$$F_1^{\text{PWBA}} = f_T^{\text{PWBA}}(Q^2) \frac{Q^2}{4|\vec{q}|} G_M^2 S(\nu, Q^2),$$

$$F_2^{\text{PWBA}} = f_T^{\text{PWBA}}(Q^2) \frac{\nu Q^4}{M_d |\vec{q}|^5} \frac{G_E^2 + \tau G_M^2}{1 + \tau} \times S(\nu, Q^2) \left( M + \frac{\nu}{2} \right)^2, \quad (26)$$

$$F_1^{\text{FSI}} = M_d f_T^{\text{FSI}}(Q^2) \sigma_T^0,$$

$$F_2^{\text{FSI}} = \frac{\nu Q^2}{|\vec{q}|^2} [f_T^{\text{FSI}}(Q^2) \sigma_T^0 + f_L^{\text{FSI}}(Q^2) \sigma_L^0],$$

where we adopted the following forms:

$$f_T^{\text{PWBA}}(Q^2) = [1 - a_1 e^{-b_1 Q^2}],$$

$$f_T^{\text{FSI}}(Q^2) = \frac{100a_2 Q^2}{(1 + b_2 Q^2)^2},$$

$$f_L^{\text{FSI}}(Q^2) = \frac{1}{\text{MeV}} \frac{1 - e^{-a_3 Q^2}}{1 + b_3 Q^2}. \quad (27)$$

We fitted the available data from  $Q^2 = 0.005$  GeV<sup>2</sup> to  $Q^2 = 3$  GeV<sup>2</sup> (see Figs. 3–10), and the resulting values of the parameters are listed in Table II.

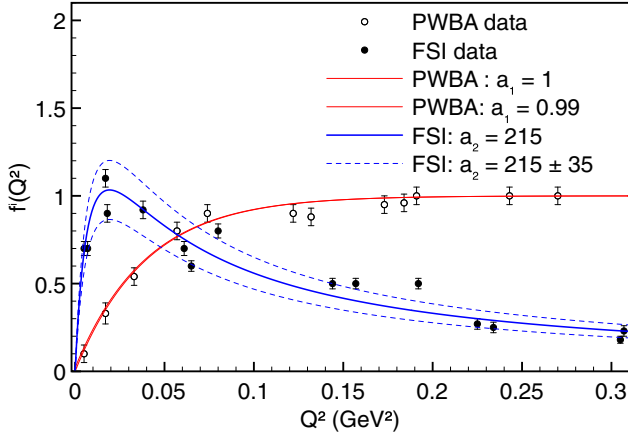


FIG. 3. (Color online) Scaling factors  $f_T^i(Q^2)$  with uncertainty thereof:  $i = \text{PWBA}$  (red solid lines), and  $i = \text{FSI}$  (blue solid line) with uncertainty thereof (thin blue short-dashed lines) plotted vs QE data as function of  $Q^2$ .

The parameter  $C_\perp$  is obtained from a fit to real photon data and the value of Baldin sum rule for real photons,

$$\alpha_E^d + \beta_M^d = \frac{2\alpha_{em}}{M_d} \int_{\nu_{th}}^{\nu_\pi} \frac{d\nu}{\nu^3} F_1^d(\nu, 0), \quad (28)$$

where  $\alpha_E^d$  and  $\beta_M^d$  are the deuteron electric and magnetic polarizabilities, respectively. There exist calculations in chiral effective field theory (EFT) by Chen *et al.* [44] and in nonrelativistic potential models, e.g., by Friar [21], that give close results that can be cast in the following form:  $\alpha_E^d = 0.633(1) \text{ fm}^3$ , and  $\beta_M^d = 0.072(5) \text{ fm}^3$ . The uncertainty in the value of the polarizabilities was obtained by averaging over the two calculations. Evaluating the Baldin integral with  $F_1^\perp$  (the only piece that does not vanish at the real photon point) leads to

$$C_\perp = 1.28(1). \quad (29)$$

Adopting these ingredients, the QE contribution of the two-photon exchange (TPE) to Lamb shift in deuterium can be calculated. We evaluated this contribution with the nucleon form factors in Kelly's parametrization [45] and using  $S(\nu, Q^2)$ ,  $S_\perp(\nu, Q^2)$  from Paris WF [46], and list the result with the uncertainty in Table I.

TABLE I. TPE corrections to the  $2S_{1/2}$  energy level in muonic deuterium in units of meV.

$\Delta \bar{E}^{el}$	-0.417(2)
$\Delta E^{\text{PWBA}}$	-1.616(739)
$\Delta E^{\text{FSI}}$	-0.391(44)
$\Delta E^\perp$	-0.322(3)
$\Delta E^{\text{hadr}}$	-0.028(2)
$\Delta E^\beta$	0.740(40)
$\Delta E^{Th}$	0.023(1)
$\Delta E_{\text{total}}$	-2.011(740)

TABLE II. The values of the parameters introduced in Eq. (27) as obtained from a fit to the deuteron QE data.

$a_1$	$b_1(\text{GeV}^{-2})$	$a_2(\text{GeV}^{-3})$
0.995(5)	25.4(6)	215(35)
$b_2(\text{GeV}^{-2})$	$a_3(\text{GeV}^{-3})$	$b_3(\text{GeV}^{-2})$
52(8)	3.5(1.5)	24.5(8.0)

#### D. Subtraction term

Following Ref. [28], we identify

$$\bar{T}_1(0, Q^2) = T_1^B(0, Q^2) - T_1^{\text{pole}}(0, Q^2) + \frac{Q^2}{e^2} \beta_M^d(0) F_\beta(Q^2), \quad (30)$$

where  $T_1^B$  ( $T_1^{\text{pole}}$ ) represent the Born (pole) contributions, respectively, and where in the polarizability term we explicitly factored out the  $Q^2$  dependence. The polarizability contribution to the  $nS$  level is given by

$$\Delta E_{n0}^\beta = 2\alpha\phi_{n0}^2(0)\beta_M^d(0) \int_0^\infty dQ^2 \frac{\gamma_1(\tau_1)}{\sqrt{Q^2}} F_\beta(Q^2), \quad (31)$$

with  $\beta_M^d(0) = 0.072(5) \text{ fm}^3$ . The  $Q^2$ -dependent form factor  $F_\beta(Q^2)$  is generally not known. We estimate it by setting  $F_\beta(Q^2) = G_C^d(Q^2)/G_C^d(0)$ , and to estimate the uncertainty we also try  $F_\beta(Q^2) = G_M^d(Q^2)/G_M^d(0)$ . The average result and uncertainty is quoted in Table I.

Finally, the subtraction function in Eq. (30) also contains the difference between the Born and pole contributions, which results from the contact two-photon deuteron interaction (Thomson term). The pointlike part of it,  $-1/4\pi M_d$  was already taken into account in atomic calculations, thus we only need to account for

$$\begin{aligned} & [T_1^B - T_1^{\text{pole}}](0, Q^2) - [T_1^{B, \text{point}} - T_1^{\text{pole, point}}](0, Q^2) \\ &= \frac{1 - G_C^2(Q^2)}{4\pi M_d}, \end{aligned} \quad (32)$$

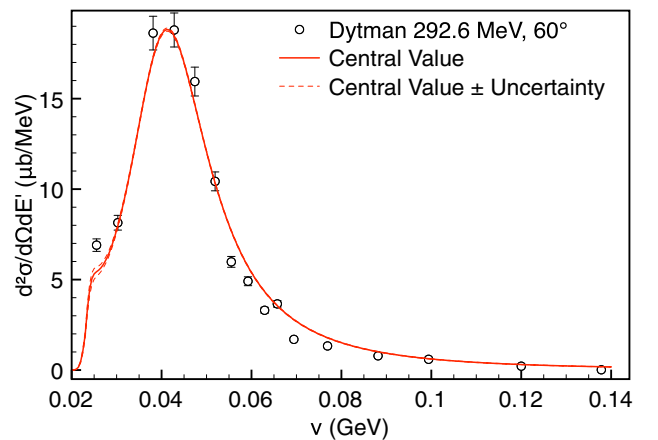


FIG. 4. (Color online) Rescaled PWBA model of Eqs. (25) and (26) vs data from Ref. [35].

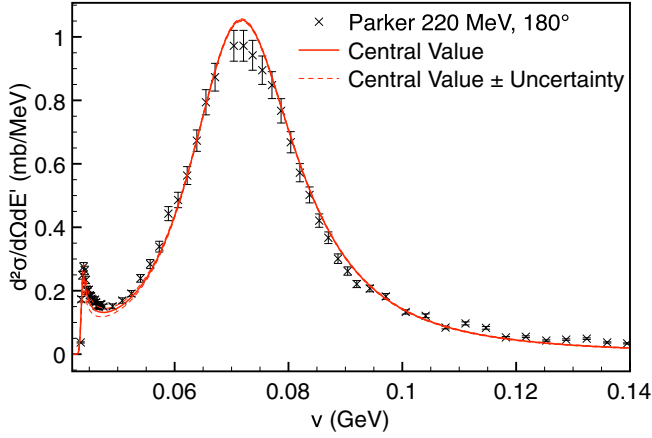


FIG. 5. (Color online) Same as in Fig. 4 vs data from Ref. [36].

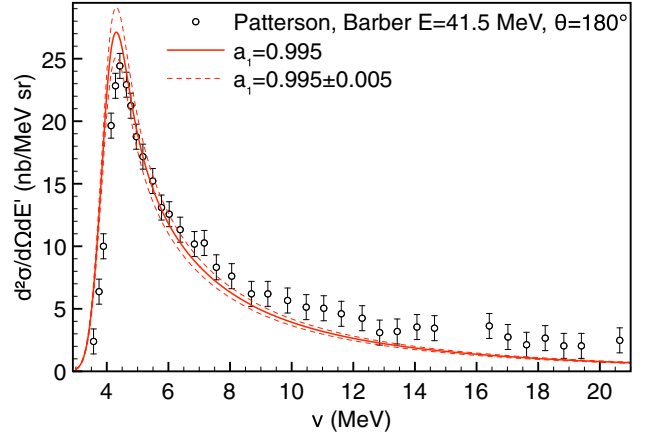


FIG. 7. (Color online) Same as in Fig. 4 vs data from Ref. [38].

thus leading to the shift of an  $S$  level,

$$\Delta E_{n0}^{Th} = \frac{2\alpha^2}{M_d} \phi_{n0}^2(0) \int_0^\infty dQ^2 \frac{\gamma_1(\tau_l)}{\sqrt{Q^2}} \frac{1 - G_C^2(Q^2)}{Q^2}. \quad (33)$$

The result of the numerical evaluation is listed in Table I.

#### IV. DISCUSSION OF RESULTS AND IMPACT OF FURTHER SCATTERING EXPERIMENTS

The total result for the  $2P - 2S$  Lamb shift obtained from the sum of all terms  $O(\alpha^5)$  due to two-photon exchange amounts to

$$\Delta E_{2P-2S} = 2.01(74) \text{ meV}. \quad (34)$$

The uncertainty of our result comes from three sources: elastic deuteron form factors, inelastic hadronic excitations, and nuclear (quasielastic) contributions. The deuteron elastic form factors have been measured over a wide  $Q^2$  range with good precision, and the error associated with different parametrizations of these data amounts to  $2 \mu\text{eV}$  or relative 2% uncertainty. The hadronic part contribution is constrained to a relative 7%, however fortunately the contribution itself is rather small, so this somewhat large relative uncertainty translates in  $2 \mu\text{eV}$  absolute uncertainty.

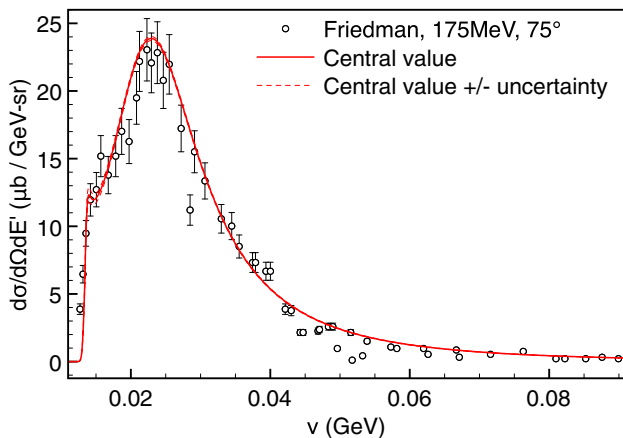


FIG. 6. (Color online) Same as in Fig. 4 vs data from Ref. [37].

At the moment, for the calculation of the subtraction contribution we rely on the  $Q^2$  dependence for the magnetic polarizability obtained from a model. A direct calculation of  $\bar{T}_1(0, Q^2)$ , for instance in chiral EFT would help reducing the corresponding uncertainty.

The largest contribution and the source of the largest uncertainty is the quasielastic piece, in particular the  $Q^2$  dependence of the inelastic structure function  $F_2(\nu, Q^2)$  in the range  $\nu \leq 10 \text{ MeV}$ ,  $Q^2 \leq 0.01 \text{ GeV}^2$  from which the dominant contribution to the Lamb shift stems. A dedicated measurement at Mainz with the existing A1 apparatus at  $E_0 = 180 \text{ MeV}$  and angles  $\theta_{\text{lab}} \geq 15^\circ$  is planned [47], and it would help somewhat to constrain the uncertainty with  $Q^2 \gtrsim 2.2 \times 10^{-3} \text{ GeV}^2$ . Going to lower energies will be possible with the new linear accelerator machine MESA at Mainz, and we include a few plots demonstrating the sensitivity to the parameter  $a_1$  in several representative kinematics in Fig. 11.

To bring the discussion to a more quantitative level, we list the projected impact of a  $d(e, e')pn$  measurement in several kinematics of A1 and MESA for the uncertainty of the dispersion calculation of the Lamb shift in Table III. For this analysis, we assumed for simplicity that the uncertainty

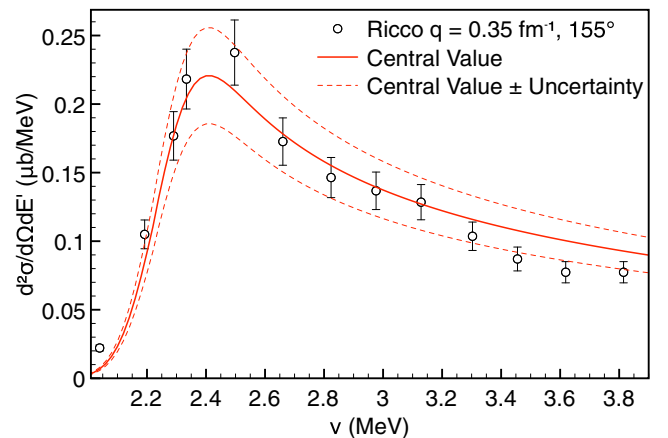


FIG. 8. (Color online) Same as in Fig. 4 vs data from Ref. [39].

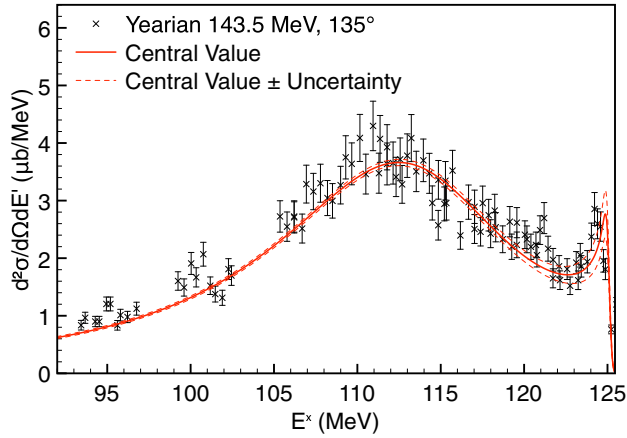


FIG. 9. (Color online) Same as in Fig. 4 vs data from Ref. [40] as function of excitation energy  $E^x$ .

of the fit will be equal to the precision of the data.<sup>1</sup> For the kinematics  $E_{\text{lab}} = 80$  MeV,  $\theta = 16^\circ$ , the uncertainty of the quasielastic contribution is reduced by a factor of 15 and the theory uncertainty starts being dominated by that due to the subtraction constant (estimated to be  $40 \mu\text{eV}$ ). It can be seen that already the next MAMI A1 runs at the lowest energy of 180 MeV and the most forward angle of  $16^\circ$  with a 2% precision have the potential to reduce the uncertainty of our dispersion calculation by at least a factor of 4. The sensitivity to the value of the parameter  $a_1$  is further enhanced at a lower energy as can be seen in the lower panel of Fig. 11. Future measurements will allow us to test other theoretical frameworks, such as potential models and EFT, as well.

Our result should be compared to those obtained by other groups [19–21,23,24,48–50]. Note that [48–50] did not perform a complete calculation and take, for instance, the nuclear polarizability correction from other works. To

<sup>1</sup>If the experimental uncertainty is dominated by the systematics this will be a correct estimate. In the opposite case the fit to 2% data will typically return an uncertainty of at most 1%.

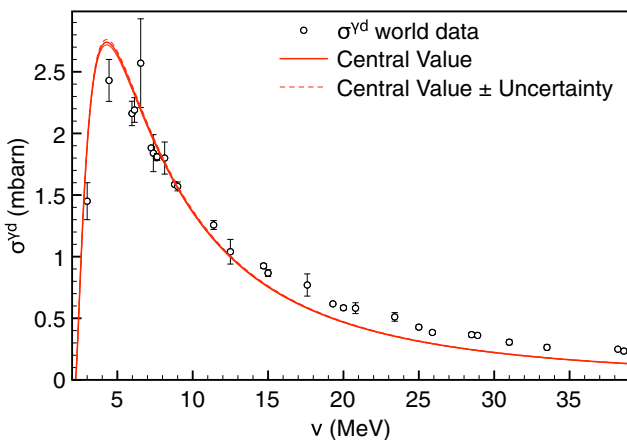


FIG. 10. (Color online) Same as in Fig. 4 vs deuteron total photoabsorption data from Refs. [41,42]. Older data compilation can be found in Ref. [43].

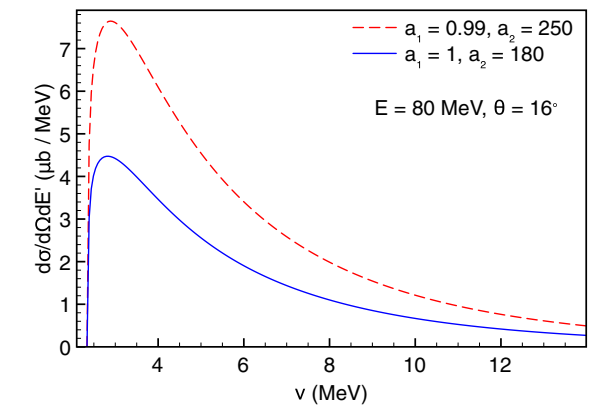
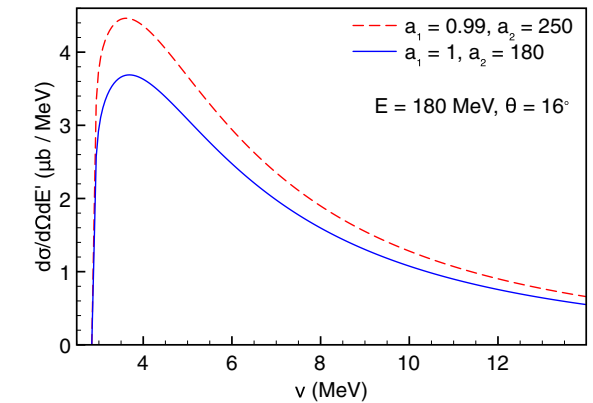
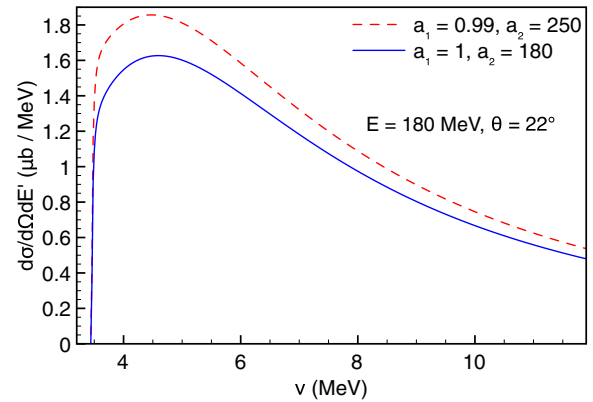
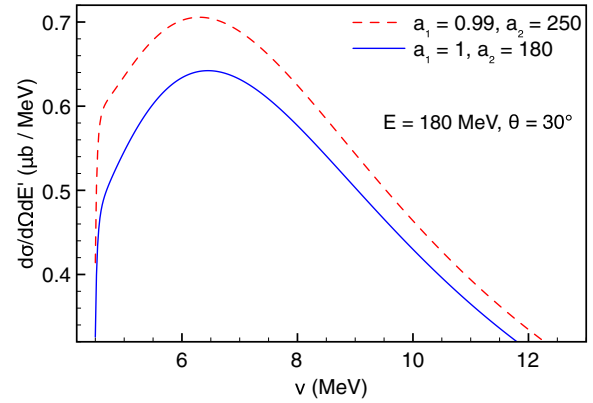


FIG. 11. (Color online) Sensitivity to the variation of the parameter  $a_1$  entering  $f_T^{\text{PWBA}}$  in the range  $[0.99, 1]$  and  $a_2$  entering  $f_T^{\text{FSI}}$  in the range  $[180, 250]$  is shown by the dashed and solid lines, respectively, in the kinematics relevant for the MAMI A1 apparatus [47] (three upper panels), and for MESA at 80 MeV (lower panel).

TABLE III. Impact of future measurements of the deuteron electrodesintegration at MAMI A1 and MESA (kinematics in the first column and experimental precision in the second column) on the theoretical uncertainty of the TPE contribution to the Lamb shift in muonic deuterium (third column) and the  $(1S - 2S)$  splitting in electronic deuterium (fourth column).

$E_{\text{lab}}, \theta_{\text{lab}}$	Expt. precision	$\delta(\Delta E_{2S-2P}^{\mu D})$ in $\mu\text{eV}$	$\delta(\Delta E_{1S-2S}^{eD})$ in kHz
180 MeV, $30^\circ$	2%	740	12
	1%	370	6
180 MeV, $22^\circ$	2%	390	6.32
	1%	195	3.16
180 MeV, $16^\circ$	2%	211	3.36
	1%	110	1.68
80 MeV, $16^\circ$	2%	67	1.08
	1%	48	0.78

facilitate the comparison, we list our results along with those obtained by other groups in Table IV. To make a sensible comparison possible we reorganized the various contributions listed in Table I as follows: ‘‘Elastic’’ denotes  $\Delta \bar{E}^{el} + \Delta E^{Th}$ , and ‘‘Nuclear’’ is sum of all nuclear contributions,  $\Delta E^{\text{PWBA}} + \Delta E^{\text{FSI}} + \Delta E^\perp + \Delta E^\beta$ .

Reference [20] quotes 1.500 meV  $2P - 2S$  correction due to the deuteron nuclear electric dipole polarizability; in Ref. [19] a result of 1.680(16) meV is obtained by considering the electric polarizability (and various corrections thereto), elastic and hadronic contributions, and magnetic polarizability. Reference [19] furthermore obtains the sum of the proton and neutron intrinsic polarizabilities to the Lamb shift in muonic deuterium by rescaling the *total* Lamb shift for muonic hydrogen,  $\Delta E_{\mu H} = 36.9 \mu\text{eV}$  obtained in Ref. [27] with the ratio  $(\mu_r^D/\mu_r^H)^3$  with the result  $\Delta E_{\mu D}^{\text{hadr.}} = 43(3) \mu\text{eV}$ . This estimate is not correct because the main contribution to  $\Delta E_{\mu H}$  is due to the elastic contribution, and only about a third of it,  $13.5 \mu\text{eV}$  comes from polarizabilities. Since proton and neutron electric polarizabilities are very close,  $\alpha_p \approx \alpha_n$ , one should expect that the result for the deuteron should be roughly equal to their sum,  $\Delta E_{\mu D}^{\text{hadr.}} \sim 2\Delta E_{\mu H} = 27 \mu\text{eV}$ . Indeed, our result (third entry in Table I) is consistent with this simple estimate,  $\Delta E_{\mu D}^{\text{hadr.}} = 28(2) \mu\text{eV}$ . This suggests that after correction the full result of Ref. [19] should be 1.665(16) meV. On the other hand, Ref. [23] estimates the Lamb shift in the zero-range approximation to be 1.912 meV (1.942 with

TABLE IV. Nuclear and nucleon structure-dependent  $O(\alpha^5)$  contributions to the  $2P - 2S$  Lamb shift in muonic deuterium as calculated by different groups, in units of meV. In case of Refs. [19,23,24] the separation of the result into ‘‘elastic’’ and ‘‘nuclear’’ contributions is not possible, and the sum of the two is quoted.

Contribution	This work	[19]	[23]	[24]	[20]	[49]
Elastic	0.394(2)					0.37
Hadronic	0.028(2)	0.043				
Nuclear	1.589(740)	1.637(16)			1.5	
Total	2.011(740)	1.680(16)	1.942	1.698		

further corrections), and quotes the result of Ref. [19] in that approximation as 1.899 meV. These numbers are close to each other, nevertheless, we point out that the differences are not small, especially compared to the uncertainty of  $16 \mu\text{eV}$  claimed in Ref. [19]. As mentioned above, the correct account of the nucleon polarizability corrections alone shifts the result of Ref. [19] by  $15 \mu\text{eV}$  that exhausts the claimed precision of the calculation. In Ref. [24] the calculation of the polarizability correction is reexamined and higher-order relativistic corrections from longitudinal and transverse two-photon exchanges were included, leading to an additional contribution of  $18 \mu\text{eV}$ .

## V. ELECTRONIC HYDROGEN

To complete the discussion, we assess the nuclear polarizability correction for the  $nS$  levels in the usual (electronic) deuterium, too. In particular, the isotopic shift measurement of  $1S - 2S$  splitting of Ref. [15] relies on the theoretical estimate according to Ref. [22],

$$\Delta E_{2S-1S}^{e-D} = 19.04(7) \text{ kHz}, \quad (35)$$

where the polarizability correction of 18.58(7) kHz and the elastic contribution of 0.46 kHz were added together. Reference [51] gives a somewhat different result,

$$\Delta E_{2S-1S}^{e-D} = 19.25 \text{ kHz}, \quad (36)$$

with the Coulomb contribution 17.24 kHz, the magnetic contribution 2.28 kHz, and the magnetic polarizability correction  $-0.27$  kHz.

Our evaluation for the  $1S - 2S$  splitting in deuterium is

$$\Delta E_{2S-1S}^{e-D} = 28.8 \pm 12.0 \text{ kHz}, \quad (37)$$

that is the sum of the elastic [0.53(1) kHz], inelastic [33.4(12.0) kHz], and subtraction [ $-4.60(3)$  kHz] contributions. The uncertainty is about half of the full result. Since for the electronic deuterium the integrals over structure functions are even more strongly weighted at low values of  $Q^2$  where no experimental information is available, the large uncertainty does not come unexpectedly. We show in Table III (fourth column) how future electron-deuteron scattering measurements can help to improve on this estimate.

Note that this uncertainty estimate exceeds the one in Eq. (34) by two orders of magnitude. However, the main uncertainty in the isotope shift given in [15] is actually due to uncertainties in other theoretical corrections, largely caused by uncertainties in parameters such as particle masses. The total radius-related energy uncertainty in [15] is 0.89 kHz. The uncertainty from the dispersive polarizability calculation is still an order of magnitude larger; using it would change the radius difference result to

$$r_E^2(d) - r_E^2(p) = 3.8274(88) \text{ fm}^2, \quad (38)$$

increasing the uncertainty by a factor of  $\sim 10$  as compared to Eq. (1). Using the CODATA value for the proton charge radius  $r_E(p) = 0.8775(51)$  fm leads us to a new extracted value of the deuteron radius,

$$r_E(d) = 2.1442(29) \text{ fm}, \quad (39)$$

that should be compared to the previous extraction [3],  $r_E(d) = 2.1424(21)$  fm. Thus, in the electron case the increase



in the polarizability uncertainty for the isotope shift makes it comparable to the existing uncertainty in the proton radius squared. Using it merely increases the uncertainty in the inferred deuteron radius by a factor of  $\sqrt{2}$ .

## VI. CONCLUSION

We conclude that in the case of deuterium, model independence that is the main objective of our approach comes at a high price. Scattering data do not constrain the behavior of structure functions, especially the longitudinal one, at low values of the momentum transfer. Microscopical nuclear calculations do a much better job in terms of intrinsic precision that typically is of order of fractions of a percent. However, in the absence of data this claimed precision is not warranted, and once new

low- $Q^2$  electrodisintegration data are available they will serve as a useful cross-check for nuclear calculations as well.

## ACKNOWLEDGMENTS

We are grateful to M. Distler, Z.-E. Meziani, V. Pascalutsa, S. Karshenboim, D. R. Phillips, J. Yang, H. Griesshammer, K. Pachucki, J. L. Friar, and S. Bacca for useful discussions. The work of M.G. and M.V. was supported by the Deutsche Forschungsgemeinschaft DFG through the Collaborative Research Center “The Low-Energy Frontier of the Standard Model” (SFB 1044) and the Cluster of Excellence “Precision Physics, Fundamental Interactions and Structure of Matter” (PRISMA). C.E.C. acknowledges support by the U.S. National Science Foundation under Grant No. PHY-1205905.

- 
- [1] R. Pohl *et al.*, *Nature (London)* **466**, 213 (2010).  
 [2] A. Antognini *et al.*, *Science* **339**, 417 (2013).  
 [3] P. J. Mohr, B. N. Taylor, and D. B. Newell, *Rev. Mod. Phys.* **80**, 633 (2008).  
 [4] J. C. Bernauer *et al.* (A1 Collaboration), *Phys. Rev. Lett.* **105**, 242001 (2010).  
 [5] A. Gasparian *et al.*, Jefferson Lab Experiment 12-11-106 (unpublished). See [http://www.jlab.org/exp\\_prog/proposals/12/C12-11-106.pdf](http://www.jlab.org/exp_prog/proposals/12/C12-11-106.pdf).  
 [6] M. Mihovilovič and H. Merkel (A1 Collaboration), *Initial State Radiation Experiment at MAMI*, edited by R. Milner, R. Carlini, and F. Maas, AIP Conf. Proc. No. 1563 (AIP, Melville, NY, 2013), p. 187.  
 [7] R. Gilman *et al.* (MUSE Collaboration), [arXiv:1303.2160](https://arxiv.org/abs/1303.2160).  
 [8] R. J. Hill and G. Paz, *Phys. Rev. Lett.* **107**, 160402 (2011).  
 [9] I. T. Lorenz, H.-W. Hammer, and U.-G. Meissner, *Eur. Phys. J. A* **48**, 151 (2012).  
 [10] G. A. Miller, *Phys. Lett.* **B718**, 1078 (2013).  
 [11] D. Tucker-Smith and I. Yavin, *Phys. Rev. D* **83**, 101702 (2011).  
 [12] B. Batell, D. McKeen, and M. Pospelov, *Phys. Rev. Lett.* **107**, 011803 (2011).  
 [13] C. E. Carlson and B. C. Rislow, *Phys. Rev. D* **86**, 035013 (2012).  
 [14] R. Pohl *et al.* (CREMA Collaboration) (private communication).  
 [15] C. G. Parthey, A. Matveev, J. Alnis, R. Pohl, T. Udem, U. D. Jentschura, N. Kolachevsky, and T. W. Hansch, *Phys. Rev. Lett.* **104**, 233001 (2010).  
 [16] A. Huber, T. Udem, B. Gross, J. Reichert, M. Kourogi, K. Pachucki, M. Weitz, and T. W. Hansch, *Phys. Rev. Lett.* **80**, 468 (1998).  
 [17] I. Sick and D. Trautmann, *Phys. Lett.* **B375**, 16 (1996).  
 [18] M. Distler and K. Griffioen (private communication).  
 [19] K. Pachucki, *Phys. Rev. Lett.* **106**, 193007 (2011).  
 [20] W. Leidemann and R. Rosenfelder, *Phys. Rev. C* **51**, 427 (1995).  
 [21] J. L. Friar, *Phys. Rev. C* **16**, 1540 (1977); J. L. Friar, J. Martorell, and D. W. L. Sprung, *Phys. Rev. A* **56**, 4579 (1997).  
 [22] J. L. Friar and G. L. Payne, *Phys. Rev. C* **55**, 2764 (1997).  
 [23] J. L. Friar, *Phys. Rev. C* **88**, 034003 (2013).  
 [24] C. Ji, N. Nevo Dinur, S. Bacca, and N. Barnea, *Phys. Rev. Lett.* **111**, 143402 (2013).  
 [25] K. Pachucki, *Phys. Rev. A* **53**, 2092 (1996).  
 [26] A. P. Martynenko, *Phys. Atom. Nucl.* **69**, 1309 (2006).  
 [27] C. E. Carlson and M. Vanderhaeghen, *Phys. Rev. A* **84**, 020102 (2011).  
 [28] M. C. Birse and J. A. McGovern, *Eur. Phys. J. A* **48**, 120 (2012).  
 [29] M. Gorchtein, T. Hobbs, J. T. Londergan, and A. P. Szczepaniak, *Phys. Rev. C* **84**, 065202 (2011).  
 [30] M. E. Christy and P. E. Bosted, *Phys. Rev. C* **81**, 055213 (2010).  
 [31] P. E. Bosted and M. E. Christy, *Phys. Rev. C* **77**, 065206 (2008).  
 [32] D. Abbott *et al.* (JLAB t20 Collaboration), *Eur. Phys. J. A* **7**, 421 (2000).  
 [33] J. Alwall and G. Ingelman, *Phys. Lett.* **B596**, 77 (2004).  
 [34] L. Durand, *Phys. Rev.* **123**, 1393 (1961).  
 [35] S. A. Dytman, A. M. Bernstein, K. I. Blomqvist, T. J. Pavel, B. P. Quinn, R. Altemus, J. S. McCarthy, G. H. Mechtel, T. S. Ueng, and R. R. Whitney, *Phys. Rev. C* **38**, 800 (1988).  
 [36] B. Parker, R. S. Hicks, A. Hotta, R. L. Huffman, G. A. Peterson, M. A. Plum, P. J. Ryan, and R. P. Singhal, *Phys. Rev. C* **34**, 2354 (1986).  
 [37] J. I. Friedman, *Phys. Rev.* **116**, 1257 (1959).  
 [38] G. A. Patterson and W. C. Barber, *Phys. Rev.* **128**, 812 (1962).  
 [39] G. Ricco, T. E. Drake, L. Katz, and H. S. Kaplan, *Phys. Rev. C* **1**, 391 (1970).  
 [40] M. R. Yearian and E. B. Hughes, *Phys. Lett.* **10**, 234 (1964).  
 [41] Y. Birenbaum, S. Kahane, and R. Moreh, *Phys. Rev. C* **32**, 1825 (1985).  
 [42] R. Bernabei, A. Incicchitti, M. Mattioli, P. Picozza, D. Prosperi, L. Casano, S. d’Angelo, M. P. De Pascale, C. Schaerf, G. Giordano *et al.*, *Phys. Rev. Lett.* **57**, 1542 (1986).  
 [43] J. Govaerts, J. L. Lucio, A. Martinez, and J. Pestieau, *Nucl. Phys.* **A368**, 409 (1981).  
 [44] J.-W. Chen, H. W. Griesshammer, M. J. Savage, and R. P. Springer, *Nucl. Phys.* **A644**, 221 (1998).  
 [45] J. J. Kelly, *Phys. Rev. C* **70**, 068202 (2004).  
 [46] M. Lacombe *et al.*, *Phys. Lett.* **B101**, 139 (1981).  
 [47] M. Distler and J. Bernauer (private communication).  
 [48] E. Borie, *Ann. Phys.* **327**, 733 (2012).  
 [49] A. P. Martynenko and R. N. Faustov, *Phys. At. Nucl.* **67**, 457 (2004).  
 [50] A. A. Krutov and A. P. Martynenko, *Phys. Rev. A* **84**, 052514 (2011).  
 [51] A. I. Milshtein, I. B. Khriplovitch, and S. S. Petrosyan, *Sov. Phys. JETP* **82**, 616 (1996) [*Zh. Eksp. Teor. Fiz.* **109**, 1146 (1996)].